

# Device Scheduling for Over-the-Air Federated Learning with Differential Privacy

Na Yan<sup>1</sup>, Kezhi Wang<sup>2</sup>, Cunhua Pan<sup>3</sup>, and Kok Keong Chai<sup>1</sup>

<sup>1</sup>School of Electronic Engineering and Computer Science, Queen Mary University of London, U.K.

<sup>2</sup>Department of Computer Science, Brunel University London, U.K.

<sup>3</sup>National Mobile Communications Research Laboratory, Southeast University, China.

Email: {n.yan, michael.chai}@qmul.ac.uk, kezhi.wang@brunel.ac.uk, and cpan@seu.edu.cn

**Abstract**—This paper proposes a device scheduling scheme for differentially private over-the-air federated learning (DP-OTA-FL), referred to as S-DPOTAFL, where user privacy is protected by channel noise. With S-DPOTAFL, the gradients are aligned by the alignment coefficient and aggregated via over-the-air computation (AirComp). By scheduling the devices with better channel conditions in the training, S-DPOTAFL avoids the problem that the alignment coefficient is limited by the device with the worst channel condition in the system. We conduct the privacy and convergence analysis to theoretically illustrate the impact of device scheduling on privacy protection and learning performance. To improve the learning accuracy, we formulate an optimization problem with the goal to minimize the optimality gap subjecting to privacy and transmit power constraints. Furthermore, we present the condition that the S-DPOTAFL performs better than the DP-OTA-FL without considering device scheduling (NoS-DPOTAFL). The effectiveness of the S-DPOTAFL is validated through simulations.

**Index Terms**—Federated learning (FL), differential privacy (DP), over-the-air computation (AirComp), device scheduling.

## I. INTRODUCTION

Federated learning (FL) [1] is a distributed machine learning (ML) framework whose goal is to train high-quality ML models without compromising users' data privacy. In FL, edge devices train a shared ML model collaboratively using their local data, with the help of a central controller, such as a base station (BS), which updates the global model and coordinates the training process. By training models locally, FL not only makes full use of the edge devices' computing power but also reduces the power consumption, latency, and privacy exposure due to the transmission of raw data. However, despite these promising benefits, FL involves the following two challenges: First, although FL avoids the direct exposure of the user's sensitive information, it still faces the risk of privacy leakage if attacking the exchanged messages [2], [3]. Second, the massive connectivities for uploading gradients via resource-limited wireless multiple access channel (MAC) result in considerable upload latency [1], [4].

Over-the-air FL (OTA-FL) [5] with differential privacy (DP) [6], referred to as DP-OTA-FL, is a promising paradigm to overcome the two challenges jointly. On the one hand, DP prevents privacy leakage of FL by introducing random noise

into the disclosed statistics (i.e., gradients or model parameters) to mask the contribution of any individual data point. On the other hand, in OTA-FL, the gradients are transmitted simultaneously via a shared wireless MAC in an uncoded way and aggregated “over-the-air” thanks to the waveform-superposition property of a MAC. The number of dimensions used for transmitting the gradients is independent of the number of devices, which makes it highly energy and bandwidth efficient compared with the traditional communication-and-computation separation method, especially when the number of devices is large [7], [8]. Furthermore, the communication efficiency could be greatly improved with analog transmission by avoiding quantization and encoding/decoding, which is very attractive for low-latency applications [9].

Some DP-OTA-FL studies [10]–[12] considered aligned OTA-FL where the gradients are aligned by an alignment coefficient during the transmission, which can ensure an unbiased gradient estimation at the BS. Specifically, in [10], artificial Gaussian noise was added to each gradient before transmitting if channel noise cannot provide sufficient privacy protection, and a static power allocation scheme was proposed to determine the scale of the artificial noise. Instead of introducing artificial noise, the work of [11] proposed a more energy-efficient strategy to guarantee DP by adjusting the transmit power. The authors of [12] investigated DP-OTA-FL in both orthogonal multiple access (OMA) and non-orthogonal multiple access (NOMA) channels and proposed adaptive power allocation schemes. Nevertheless, all the above works considered the full device participation, and therefore the alignment coefficient is limited by the device with the worst channel condition in the system. Consequently, the signal-to-noise ratio (SNR) of the FL system may be very low, which harms the learning performance. On the other hand, some studies [13], [14] proposed the misaligned OTA-FL to overcome the above issue. However, it normally results in biased estimates of the averaging gradients, which may also result in a less accurate model.

Against the above background, a device scheduling scheme for aligned DP-OTA-FL, referred to as S-DPOTAFL, is proposed to improve the learning performance with consideration of privacy protection. By scheduling the devices with better channel conditions to participate in the training, S-DPOTAFL

can overcome the problem that the alignment coefficients is too small in DP-OTA-FL without device scheduling (NoS-DPOTAFL) [10]. The privacy and convergence analysis are conducted to demonstrate the impact of device scheduling on privacy protection and learning performance. To minimize the impact of device scheduling on training process, we formulate an optimization problem aiming to minimize the optimity gap subjecting to privacy protection and transmit power constraints. We also present the situation that S-DPOTAFL can perform better than NoS-DPOTAFL. The performance of the proposed S-DPOTAFL is evaluated through simulations by comparing it with NoS-DPOTAFL.

## II. SYSTEM MODEL AND PRELIMINARIES

As shown in Fig. 1, we consider an FL system where  $N$  edge devices, indexed by  $\mathcal{N}$ , and a BS collaboratively train a model. Assume that the BS is curious and attempts to probe sensitive information from the received gradient. In the S-SPOTAFL framework, we select those devices whose privacy can be guaranteed by channel noise to participate in training.

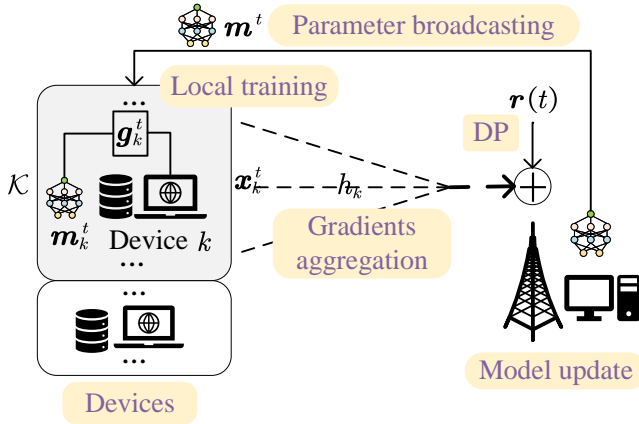


Fig. 1. Differentially private OTA-FL with device scheduling.

### A. Federated Learning

Assume that each device of index  $k \in \mathcal{N}$  stores a local dataset  $\mathcal{D}_k$  which contains  $D_k$  pairs of training samples  $(\mathbf{u}, v)$  where  $\mathbf{u}$  is the raw data and  $v$  is the corresponding label. For simplicity, we assume that  $D_1 = \dots = D_N$ . Mathematically, the goal of an FL task is to obtain the model parameter that can minimize the loss function given as follows:

$$\min_{\mathbf{m}} L(\mathbf{m}) = \frac{1}{N} \sum_{k=1}^N L_k(\mathbf{m}), \quad (1)$$

where  $\mathbf{m} \in \mathbb{R}^d$  is the model parameter to be optimized. More specifically, the objective function of device  $k$  is defined as follows:

$$L_k(\mathbf{m}) = \frac{1}{D_k} \sum_{(\mathbf{u}, v) \in \mathcal{D}_k} l(\mathbf{m}; (\mathbf{u}, v)), \quad (2)$$

where  $l(\mathbf{m}; (\mathbf{u}, v))$  is an empirical loss function defined by learning task, quantifying the loss of  $\mathbf{m}$  at sample  $(\mathbf{u}, v)$ .

To solve the problem in (1), gradient descent (GD) can be applied. The main procedure of a general GD taking round  $t+1$  as an example is given as follows: *Parameters broadcasting*: At the beginning of the training round, the BS broadcasts the latest global model parameter  $\mathbf{m}^t$  to all the devices. *Local training*: Each device first performs the initialization of the local model by setting the received global model parameter as the local model parameter, i.e.,  $\mathbf{m}_k^t = \mathbf{m}^t, \forall k$ . Then, each device computes the gradient by

$$\mathbf{g}_k^t \triangleq \nabla L_k(\mathbf{m}_k^t) = \frac{1}{D_k} \sum_{(\mathbf{u}, v) \in \mathcal{D}_k} \nabla l(\mathbf{m}_k^t; (\mathbf{u}, v)), \quad (3)$$

which is sent to the BS for aggregation. *Gradients aggregation*: Upon receiving all the gradients from the participants, the BS makes an aggregation of the received gradients as follows:

$$\mathbf{g}^t = \frac{1}{N} \sum_{k=1}^N \mathbf{g}_k^t. \quad (4)$$

*Model update*: The BS performs global model update as follows:

$$\mathbf{m}^{t+1} = \mathbf{m}^t - \tau \mathbf{g}^t, \quad (5)$$

where  $\tau$  is the learning rate (also termed as step size in GD). The above iteration steps are repeated until a certain training termination condition is met.

### B. Differential Privacy

DP [6] is defined on the conception of the adjacent dataset, which guarantees the probability that any two adjacent datasets output the same result is less than a constant with the help of adding random noise. More specifically, DP quantifies information leakage in FL by measuring the sensitivity of the the gradients to the change of a single data point in the input dataset. The basic definition of  $(\epsilon, \xi)$ -DP is given as follows.

**Definition 1.**  $(\epsilon, \xi)$ -DP [6]: A randomized mechanism  $\mathcal{O}$  guarantees  $(\epsilon, \xi)$ -DP if for two adjacent datasets  $\mathcal{D}, \mathcal{D}'$  differing in one sample, and measurable output space  $\mathcal{Q}$  of  $\mathcal{O}$ , it satisfies,

$$\Pr[\mathcal{O}(\mathcal{D}) \in \mathcal{Q}] \leq e^\epsilon \Pr[\mathcal{O}(\mathcal{D}') \in \mathcal{Q}] + \xi. \quad (6)$$

The additive term  $\xi$  allows for breaching  $\epsilon$ -DP with the probability  $\xi$  while  $\epsilon$  denotes the protection level and a smaller  $\epsilon$  means a higher privacy preservation level. Specifically, the Gaussian DP mechanism which guarantees privacy by adding artificial Gaussian noise is introduced as follows.

**Definition 2.** Gaussian mechanism [6]: A mechanism  $\mathcal{O}$  is called as a Gaussian mechanism, which alters the output of another algorithm  $\mathcal{L} : \mathcal{D} \rightarrow \mathcal{Q}$  by adding Gaussian noise, i.e.,

$$\mathcal{O}(\mathcal{D}) = \mathcal{L}(\mathcal{D}) + \mathcal{N}(0, \sigma^2 \mathbf{I}_d). \quad (7)$$

Gaussian mechanism  $\mathcal{O}$  guarantees  $(\epsilon, \xi)$ -DP with  $\epsilon = \frac{\Delta S}{\sigma} \sqrt{2 \ln \left( \frac{1.25}{\xi} \right)}$  where  $\Delta S \triangleq \max_{\mathcal{D}, \mathcal{D}'} \|\mathcal{L}(\mathcal{D}) - \mathcal{L}(\mathcal{D}')\|_2$  is the

sensitivity of the algorithm  $\mathcal{L}$  quantifying the sensitivity of the algorithm  $\mathcal{L}$  to the change of a single data point.

### III. DP-OTA-FL WITH DEVICE SCHEDULING

Inspired by [10], we consider the aligned OTA-FL. To avoid the problem that the alignment coefficient is limited by the device with the worst channel condition in the system, we propose the S-DPOTAF. The details are described as follows.

Assume that  $P_k$  is the maximum transmission power of device  $k$  and  $\mathcal{K} \subseteq \mathcal{N}$  is the set of the scheduled devices. The signal sent from device  $k$  in training round  $t + 1$  is given as:

$$\mathbf{x}_k^t = e^{-j\psi_k} \left[ \frac{\sqrt{\varphi_k P_k}}{\varpi} \mathbf{g}_k^t \right], \forall k \in \mathcal{K}, \quad (8)$$

where  $e^{-j\psi_k}$  is the local phase correction performed by the device  $k$ .  $\varphi_k \in [0, 1]$  is the power scaling factor and we also assume  $\|\mathbf{g}_k^t\|_2 \leq \varpi$  so that  $\mathbb{E}[\|\mathbf{x}\|_2^2] \leq P_k$ . Consequently, the received signal at the BS is

$$\begin{aligned} \mathbf{y}(t) &= \sum_{k \in \mathcal{K}} h_k \mathbf{x}_k^t + \mathbf{r}(t) \\ &= \sum_{k \in \mathcal{K}} |h_k| \frac{\sqrt{\varphi_k P_k}}{\varpi} \mathbf{g}_k^t + \mathbf{r}(t), \end{aligned} \quad (9)$$

where  $h_k = |h_k| e^{j\psi_k}$  is the complex-valued time-invariant channel coefficient between device  $k$  and the BS.  $\mathbf{r}(t) \sim \mathcal{N}(0, \sigma^2 \mathbf{I}_d)$  is the received noise at the BS, which is employed to prevent privacy leakage in this paper.

In order to obtain an unbiased estimate of the averaging gradient, all users adjust the coefficients  $\varphi_k$  to align the transmitted local gradient by the alignment coefficient  $\nu$  as follows:

$$|h_k| \frac{\sqrt{\varphi_k P_k}}{\varpi} = \nu, \forall k \in \mathcal{K}. \quad (10)$$

It thus follows (10) that

$$\varphi_k = \frac{\nu^2 \varpi^2}{|h_k|^2 P_k}, \forall k \in \mathcal{K}. \quad (11)$$

To make sure that  $\varphi_k \leq 1$ , the following condition needs to be satisfied:

$$\nu \leq \frac{\min_{s \in \mathcal{K}} \{|h_s| \sqrt{P_s}\}}{\varpi}. \quad (12)$$

According to such aggregation scheme described above, the received signal at the BS in (9) can be simplified as:

$$\mathbf{y}(t) = \nu \sum_{k \in \mathcal{K}} \mathbf{g}_k^t + \mathbf{r}(t). \quad (13)$$

It can be learned that a smaller  $\nu$  results in a low SNR of the FL system. In order to estimate the averaging gradient, the BS performs post-processing as follows:

$$\tilde{\mathbf{g}}^t = \frac{1}{|\mathcal{K}| \nu} \mathbf{y}(t) = \frac{1}{|\mathcal{K}|} \sum_{k \in \mathcal{K}} \mathbf{g}_k^t + \frac{1}{|\mathcal{K}| \nu} \mathbf{r}(t), \quad (14)$$

which is finally used to update global model as follows:

$$\mathbf{m}^{t+1} = \mathbf{m}^t - \tau \tilde{\mathbf{g}}^t. \quad (15)$$

## IV. PRIVACY AND CONVERGENCE ANALYSIS AND PROBLEM FORMULATION

To illustrate the impact of device scheduling on privacy protection and learning performance, we conduct privacy and convergence analysis. Then, based on these analytical results, we formulate an optimization problem to minimize the optimality gap with consideration of privacy and transmit power constraints.

### A. Privacy and Convergence Analysis

1) *Assumptions*: For analysis purposes, we provide the following assumptions first.

**Assumption 1.** *The expected squared norm of each gradient is bounded:*

$$\mathbb{E}[\|\mathbf{g}_k^t\|_2] \leq \varpi. \quad (16)$$

**Assumption 2.** *Assume that  $L(\cdot)$  is  $\zeta$ -smooth, i.e., for all  $\mathbf{l}'$  and  $\mathbf{l}$ , one has*

$$L(\mathbf{l}') - L(\mathbf{l}) \leq (\mathbf{l}' - \mathbf{l})^\top \nabla L(\mathbf{l}) + \frac{\zeta}{2} \|\mathbf{l}' - \mathbf{l}\|_2^2. \quad (17)$$

**Assumption 3.** *Assume that  $L(\cdot)$  satisfies Polyak-Lojasiewicz inequality, i.e., for all  $\mathbf{l}$ , there is a constant  $\rho \geq 0$  satisfying,*

$$\|\nabla L(\mathbf{l})\|_2^2 \geq 2\rho (L(\mathbf{l}) - L(\mathbf{l}^*)). \quad (18)$$

2) *Privacy analysis*: We here present the privacy analysis of the S-DPOTAF.

**Lemma 1.** *Assume that Assumption 1 holds. S-DPOTAF guarantees  $(\epsilon_k, \xi)$ -DP of device  $k \in \mathcal{K}$  where*

$$\epsilon_k = \frac{2\varpi\nu}{\sigma} \cdot \phi, \quad (19)$$

where  $\phi = \sqrt{2 \ln \frac{1.25}{\xi}}$ .

*Proof*: Here we use index  $m$  instead of  $k$  to avoid confusion between the specific index of device  $k$  and the notation  $k$  in the summation. Assume that  $\mathcal{D}_m$  and  $\mathcal{D}'_m$  are two adjacent datasets differing in one sample.  $\mathbf{y}'(t)$  is the received signal at the BS, which only differs in one gradient with  $\mathbf{y}(t)$ . The gradient  $(\mathbf{g}_m^t)'$  from device  $m$  in  $\mathbf{y}'(t)$  is obtained based on  $\mathcal{D}'_m$ . Based on the definition of sensitivity and Assumption 1, one has

$$\begin{aligned} \Delta S_m &\triangleq \max_{\mathcal{D}_m, \mathcal{D}'_m} \|\mathbf{y}(t) - \mathbf{y}'(t)\|_2 = \max_{\mathcal{D}_m, \mathcal{D}'_m} \left\| \nu (\mathbf{g}_m^t - (\mathbf{g}_m^t)') \right\|_2 \\ &= \nu \left\| \mathbf{g}_m^t - (\mathbf{g}_m^t)' \right\|_2 \stackrel{(a)}{\leq} 2\varpi\nu, \end{aligned} \quad (20)$$

where (a) is from triangular inequality and Assumption 1. According to Definition 2 and the above result, one completes the proof of Lemma 1 by replacing  $m$  with  $k$ . ■

Lemma 1 shows the impact of the alignment coefficient on privacy leakage. More specifically, a smaller alignment coefficient  $\nu$  leads to less privacy leakage.

**Remark 1.** *Note that when the “=” in (19) is replaced by “≤”, it indicates a stronger privacy protection so it still satisfies  $(\epsilon_k, \xi)$ -DP.*

3) *Convergence analysis*: We here present the results of convergence analysis to show the impact of devices scheduling and alignment coefficient on the training process. Assume that the training process terminates after  $T$  rounds and  $\mathbf{m}^T$  is the obtained model and  $\mathbf{m}^*$  is the optimal global model. Then, we have the following results.

**Theorem 1.** *Given the learning rate  $\tau = \frac{1}{\zeta}$ , the upper bound of the optimality gap  $\mathbb{E}[L(\mathbf{m}^T) - L(\mathbf{m}^*)]$  is given by*

$$\begin{aligned} & \mathbb{E}[L(\mathbf{m}^T) - L(\mathbf{m}^*)] \\ & \leq \eta^{T-1} \mathbb{E}[L(\mathbf{m}^0) - L(\mathbf{m}^*)] + \frac{\Phi(\mathcal{K}, \nu)}{2\zeta} \frac{1 - \eta^{T-1}}{1 - \eta}, \end{aligned} \quad (21)$$

where

$$\eta = 1 - \frac{\rho}{\zeta}, \quad (22)$$

and

$$\Phi(\mathcal{K}, \nu) = 4\varpi^2 \left(1 - \frac{|\mathcal{K}|}{N}\right)^2 + \frac{d\sigma^2}{|\mathcal{K}|^2 \nu^2}, \quad (23)$$

which characterizes the impact of alignment coefficient and device scheduling on the optimality gap. The expectation is with respect to the randomness of Gaussian noise.

*Proof*: Please refer to Appendix A.  $\blacksquare$

The first term on the right-hand side of the optimality gap is the initial gap which decreases with  $T$  as  $\eta \leq 1$ . The second term reveals the impact of alignment coefficient and device scheduling on learning performance. More specifically, the larger number of scheduled devices and alignment coefficient benefit the training process. It can be understood by observing (13) that the channel noise makes smaller distortion to the gradients when more devices are involved. Additionally, a larger alignment coefficient means a higher SNR of the system. From (12), we can learn that the alignment coefficient  $\nu$  is limited by the scheduled device with the worst channel condition, i.e.,  $\min_{s \in \mathcal{K}} \{|h_s|^2 P_s\}$ . Therefore, an appropriate device selection is significant for improving learning performance while preserving privacy.

Based on Theorem 1, we can also derive the optimality gap of an FL system with full device participation and a noise-free channel.

**Corollary 1.** *Given the learning rate  $\tau = \frac{1}{\zeta}$ , the upper bound of the optimality gap  $\mathbb{E}[L(\mathbf{m}^T) - L(\mathbf{m}^*)]$  of the FL algorithm without considering noise and device scheduling is*

$$\begin{aligned} & \mathbb{E}[L(\mathbf{m}^T) - L(\mathbf{m}^*)] \\ & \leq \left(1 - \frac{\rho}{\zeta}\right)^{T-1} \mathbb{E}[L(\mathbf{m}^0) - L(\mathbf{m}^*)]. \end{aligned} \quad (24)$$

*Proof*: Since the FL algorithms do not consider the noise and device selection, we have  $\sigma = 0$  and  $|\mathcal{K}| = N$ . Hence,  $4\varpi^2 \left(1 - \frac{|\mathcal{K}|}{N}\right)^2 + \frac{d\sigma^2}{|\mathcal{K}|^2 \nu^2} = 0$ . Then (24) can be derived based on (21).  $\blacksquare$

From Corollary 1, we can observe that, if we do not consider the noise, the FL algorithm with full device participation will

converge to the optimal global FL model without any gaps. This result corresponds to the results in the existing works [15], [16].

### B. Optimization Problem for Device Scheduling

In this section, our goal is to minimize the optimality gap via the selection of participants and alignment coefficient considering privacy preservation. Assume that each device has the same requirement of privacy protection, i.e.,  $(\epsilon, \xi)$ . By omitting the terms that are irrelevant to device scheduling and alignment coefficient, the optimization problem is formulated as follows:

$$\mathbf{P1.} \quad \min_{\mathcal{K}, \nu} \left\{ 4\varpi^2 \left(1 - \frac{|\mathcal{K}|}{N}\right)^2 + \frac{d\sigma^2}{|\mathcal{K}|^2 \nu^2} \right\} \quad (25)$$

$$\text{s.t.} \quad \mathcal{K} \subseteq \mathcal{N}, \quad (25a)$$

$$\nu \leq \frac{\min_{s \in \mathcal{K}} \{|h_s| \sqrt{P_s}\}}{\varpi}, \quad (25b)$$

$$\frac{2\varpi\nu}{\sigma} \cdot \phi \leq \epsilon. \quad (25c)$$

Constraint (25b) implies that the alignment coefficient should ensure that  $\varphi_k \leq 1$  as mentioned in (12). Constraint (25c) is privacy requirement. By defining  $\theta = \varpi\nu$  and  $c_{|\mathcal{K}|} = \min_{s \in \mathcal{K}} \{|h_s| \sqrt{P_s}\}$ , Problem P1 can be equivalently rewritten as:

$$\mathbf{P2.} \quad \min_{\mathcal{K}, \theta} \left\{ 4 \left(1 - \frac{|\mathcal{K}|}{N}\right)^2 + \frac{d\sigma^2}{|\mathcal{K}|^2 \theta^2} \right\} \quad (26)$$

$$\text{s.t.} \quad \mathcal{K} \subseteq \mathcal{N}, \quad (26a)$$

$$\theta \leq \min \left\{ c_{|\mathcal{K}|}, \frac{\epsilon\sigma}{2\phi} \right\}. \quad (26b)$$

Assume that the elements in  $\mathbf{c} = [c_1, \dots, c_i, \dots, c_N]$  where  $c_i = |h_i| \sqrt{P_i}$  are sorted in ascending order. By observing the objective function, we learn that larger  $|\mathcal{K}|$  and  $\theta$  yields a better objective function value. However,  $\theta$  is equivalent to the threshold at which the device is qualified. As  $\theta$  increases, the value of  $|\mathcal{K}|$  decreases. Conversely, a larger  $|\mathcal{K}|$  leads to a smaller  $\theta$ . Therefore, there is a tradeoff between  $\theta$  and  $|\mathcal{K}|$ .

For the clarity, we give the solution in two cases: 1)  $c_1 > \frac{\epsilon\sigma}{2\phi}$ ; 2)  $c_1 \leq \frac{\epsilon\sigma}{2\phi}$  as follows:

1) *In the case that  $c_1 > \frac{\epsilon\sigma}{2\phi}$* : Constraint (26b) can be rewritten as  $\theta \leq \frac{\epsilon\sigma}{2\phi}$ . Then, we have the optimal solution as follows.

**Lemma 2.** *The optimal solution to P2 when  $c_1 > \frac{\epsilon\sigma}{2\phi}$  is*

$$\theta = \frac{\epsilon\sigma}{2\phi}, \quad \mathcal{K} = \mathcal{N}, \quad (27)$$

in which case S-SPOTAFL is equivalent to NoS-DPOTAFL.

*Proof*: Firstly, to achieve a larger  $\theta$ , we have  $\theta = \frac{\epsilon\sigma}{2\phi}$ . On the other hand, all the  $k$  with  $c_k \geq \frac{\epsilon\sigma}{2\phi}$  should be selected to achieve a larger  $|\mathcal{K}|$ , i.e., a better value of objective function. Since  $\frac{\epsilon\sigma}{2\phi} < c_1 \leq c_k, \forall k \in \mathcal{N}$ , we have  $\mathcal{K} = \mathcal{N}$ . This completes the proof of Lemma 2.  $\blacksquare$

2) In the case that  $c_1 \leq \frac{\epsilon\sigma}{2\phi}$ , we define

$$\mathcal{Q} = \left\{ k \mid c_1 \leq c_k < \frac{\epsilon\sigma}{2\phi} \right\}. \quad (28)$$

Then, we have  $c_{|\mathcal{Q}|} < \frac{\epsilon\sigma}{2\phi} \leq c_{|\mathcal{Q}|+1}$ . Constraint (26b) can be discussed in two cases: (1)  $\theta \leq c_{[k]} = c_k, k \in \mathcal{Q}$ ; (2)  $\theta \leq \frac{\epsilon\sigma}{2\phi}$ . Then, we have the following results.

**Lemma 3.** *The minimum value of  $|\mathcal{K}|$  is  $N - |\mathcal{Q}|$ . The relationship between the potential optimal solution pairs, i.e.,  $|\mathcal{K}|$  and  $\theta$ , as shown in Fig. 2 can be given by*

$$\theta = \begin{cases} c_{N-|\mathcal{K}|+1}, & \text{if } |\mathcal{K}| \geq N - |\mathcal{Q}| + 1 \\ \frac{\epsilon\sigma}{2\phi}, & \text{if } |\mathcal{K}| = N - |\mathcal{Q}| \end{cases}. \quad (29)$$

*Proof:* Firstly, given a value of  $|\mathcal{K}| \geq N - |\mathcal{Q}| + 1$ , the largest  $c_{[k]}$  that can be achieved is  $c_{N-|\mathcal{K}|+1}$ . To achieve a larger  $\theta$ , we have  $\theta = c_{N-|\mathcal{K}|+1}$ . The largest feasible value of  $\theta$  is  $\frac{\epsilon\sigma}{2\phi}$ , at which  $|\mathcal{K}|$  achieves the minimum value  $N - |\mathcal{Q}|$ . Then, we complete the proof of Lemma 3. ■

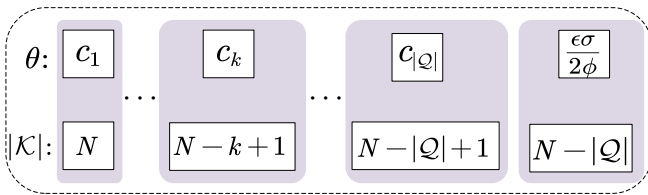


Fig. 2. The relationship between the potential optimal  $|\mathcal{K}|$  and  $\theta$ .

Lemma 3 offers an important insight that each  $\theta$  corresponds to a  $|\mathcal{K}|$ . Then, the potential solutions to **P2** can be obtained as follows.

**Lemma 4.** *There are  $|\mathcal{Q}| + 1$  closed-form solutions which may be the globally optimal solution. The  $i$ -th,  $1 \leq i \leq |\mathcal{Q}|$ , possible solution  $\theta_i$  and  $\mathcal{K}_i$  and is given by*

$$\theta_i = c_i, \quad \mathcal{K}_i = \{k \mid c_k \geq c_i\}, \quad (30)$$

and the possible solution  $\theta_{|\mathcal{Q}|+1}$ ,  $\mathcal{K}_{|\mathcal{Q}|+1}$  is

$$\theta_{|\mathcal{Q}|+1} = \frac{\epsilon\sigma}{2\phi}, \quad \mathcal{K}_{|\mathcal{Q}|+1} = \left\{ k \mid c_k \geq \frac{\epsilon\sigma}{2\phi} \right\}. \quad (31)$$

*Proof:* Firstly, there are  $|\mathcal{Q}|$  elements in  $\mathcal{Q}$ , which are the potential value of  $c_{[k]}$ , i.e.,  $\theta$ . It thus following Lemma 3 that there are  $|\mathcal{Q}|$  pairs of  $\theta$  and  $|\mathcal{K}|$ , i.e.,  $|\mathcal{Q}|$  potential optimal solutions, which may achieve the best performance. Specifically, the  $i$ -th solution corresponds to the setting that  $\theta_i = c_i$  and  $|\mathcal{K}| = N - i + 1$ . In this case,  $\mathcal{K}_i = \{i, \dots, N\}$ , i.e.,  $\mathcal{K}_i = \{k \mid c_k \geq c_i\}$ . Additionally,  $\theta = \frac{\epsilon\sigma}{2\phi}$  is the  $|\mathcal{Q}| + 1$ -th solution, in which  $\mathcal{K}_{|\mathcal{Q}|+1} = \left\{ k \mid c_k \geq \frac{\epsilon\sigma}{2\phi} \right\}$ . Then, we complete the proof of Lemma 4. ■

Based on Lemma 4, we can perform the one-dimension search method to obtain the optimal solution. The optimal solution to Problem **P2** is  $\mathcal{K}^*, \theta^*$  where

$$\mathcal{K}^*, \theta^* = \arg \min_{1 \leq i \leq |\mathcal{Q}|+1} \{\Psi(\mathcal{K}_i, \theta_i)\}, \quad (32)$$

where  $\Psi(\mathcal{K}_i, \theta_i) = 4 \left(1 - \frac{|\mathcal{K}_i|}{N}\right)^2 + \frac{d\sigma^2}{|\mathcal{K}_i|^2\theta_i^2}$ .

We next present the situation that S-DPOTA-FL performs better than NoS-DPOTAFL. Since S-DPOTA-FL is equivalent to NoS-DPOTAFL when  $c_1 > \frac{\epsilon\sigma}{2\phi}$ , we only consider the case that  $c_1 \leq \frac{\epsilon\sigma}{2\phi}$ .

**Lemma 5.** *Assume that  $c_1 \leq \frac{\epsilon\sigma}{2\phi}$ . S-DPOTAFL performs better than NoS-DPOTAFL when the following condition is satisfied:*

$$|\mathcal{K}| \theta \geq \frac{1}{\sqrt{\frac{1}{N^2 c_1^2} - \frac{4}{d\sigma^2}}}. \quad (33)$$

*Proof:* NoS-DPOTAFL is equivalent to the solution that  $\theta = c_1$  and  $\mathcal{K} = \mathcal{N}$ , in which case, the value of objective function is  $\frac{d\sigma^2}{N^2 c_1^2}$ . By solving  $4 + \frac{d\sigma^2}{|\mathcal{K}|^2 \theta^2} \leq \frac{d\sigma^2}{N^2 c_1^2}$ , we complete the proof of Lemma 5. ■

## V. SIMULATION RESULTS

We evaluate the effectiveness of the S-DPOTAFL by training a convolutional neural network (CNN) on the popular MNIST dataset. In particular, CNN consists of two  $5 \times 5$  convolution layers with the rectified linear unit (ReLU) activation. The two convolution layers have 10 and 20 channels respectively, and each layer has  $2 \times 2$  max pooling, a fully-connected layer with 50 units and ReLU activation, and a log-softmax output layer, in which case  $d = 21840$ . The learning rate is set to  $\eta = 0.1$ . We assume that each device has the same transmit power  $P$  and the minimal channel gain  $|h_k|$  is set to 0.1. The privacy level is set to  $(\epsilon, \xi) = (10, 0.1)$  and  $\sigma = 1$ .

In Fig. 3, we plot the testing accuracy of the S-DPOTAFL and NoS-DPOTAFL with different  $P$  where  $N = 50$ . It can be observed that the superiority of the S-DPOTAFL is significant when  $P$  is relatively smaller. In the cases that  $P$  is small, although all the devices are involved in training in the NoS-DPOTAFL, the alignment coefficient in the NoS-DPOTAFL is very small, which results in a quite low SNR of the FL system. Additionally, we can learn that the performance gap between NoS-DPOTAFL and S-DPOTAFL decreases as  $P$  increases. In particular, the S-DPOTAFL achieves the same accuracy as the NoS-DPOTAFL with  $P = 200$ . This is because when  $P = 200$ , we have  $c_1 > \frac{\epsilon\sigma}{2\phi}$ , in which case the optimal solution to the S-DPOTAFL is equivalent to the NoS-DPOTAFL as shown in Lemma 2.

Fig. 4 plots the testing accuracy of the S-DPOTAFL and NoS-DPOTAFL with different  $N$  where  $P = 25$ . The S-DPOTAFL performs better than the NoS-DPOTAFL in all the cases. The superiority of the S-DPOTAFL is particularly noticeable in the case that  $N = 25$  because both the number of participants and the alignment coefficient are relatively small for the NoS-DPOTAFL, while the alignment coefficient in the S-DPOTAFL is larger by selecting the devices with better channel conditions. The performance of the NoS-DPOTAFL is improved as  $N$  grows because including more devices means less noise distortion to the aggregated gradients given a fixed  $c_1$ .

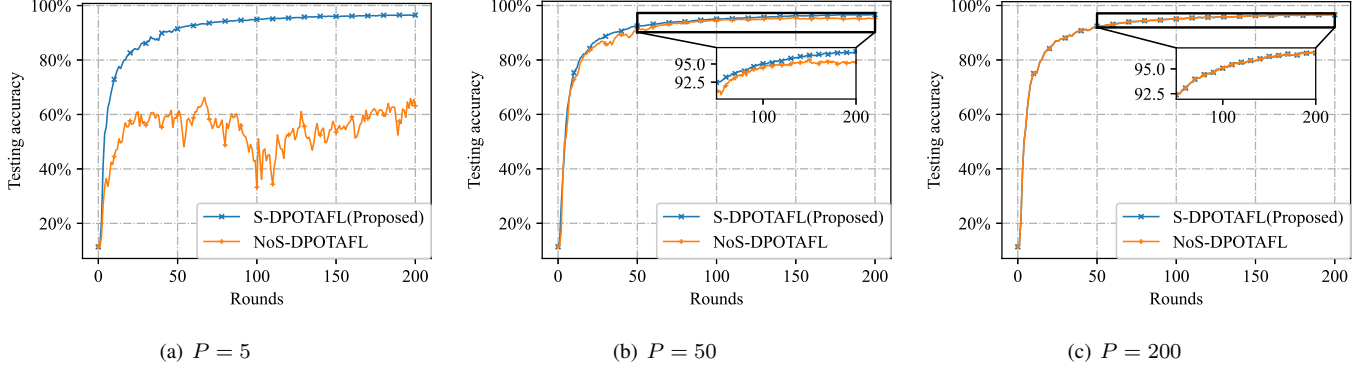


Fig. 3. Testing accuracy of the S-DPOTAFL and NoS-DPOTAFL with different  $P$ .

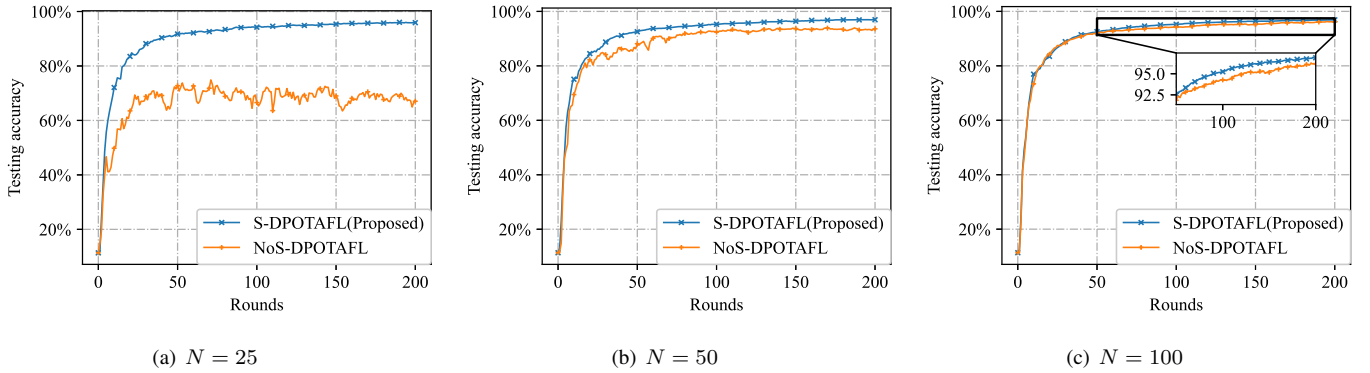


Fig. 4. Testing accuracy of the S-DPOTAFL and NoS-DPOTAFL with different  $N$ .

From all the results above, we conclude that with the small-scale FL systems where the number and the power of devices are small, the S-DPOTAFL is more useful than the NoS-DPOTAFL.

## VI. CONCLUSION

The device scheduling problem for the aligned DP-OTA-FL system has been studied in this work. The privacy and convergence analysis are conducted. We have formulated an optimization problem to minimize the optimality gap considering privacy protection. The closed-form solution has been derived and we have also obtained the scenarios that the S-DPOTAFL performs better than the NoS-DPOTAFL.

### APPENDIX A PROOF OF CONVERGENCE ANALYSIS

Recalling that

$$\mathbf{m}^{t+1} = \mathbf{m}^t - \tau (\nabla L(\mathbf{m}^t) + \mathbf{e}^t), \quad (34)$$

where

$$\mathbf{e}^t = \frac{1}{|\mathcal{K}|} \sum_{k \in \mathcal{K}} \mathbf{g}_k^t + \frac{1}{|\mathcal{K}| \nu} \mathbf{r}(t) - \nabla L(\mathbf{m}^t), \quad (35)$$

It thus following that

$$\begin{aligned} & \mathbb{E}[L(\mathbf{m}^{t+1})] - \mathbb{E}[L(\mathbf{m}^t)] \\ & \stackrel{(a)}{\leq} -\tau \mathbb{E}[\langle \nabla L(\mathbf{m}^t), \nabla L(\mathbf{m}^t) + \mathbf{e}^t \rangle] \\ & \quad + \frac{\tau^2 \zeta}{2} \mathbb{E}[\|\nabla L(\mathbf{m}^t) + \mathbf{e}^t\|_2^2] \\ & = -\tau \langle \nabla L(\mathbf{m}^t), \nabla L(\mathbf{m}^t) \rangle - \tau \langle \nabla L(\mathbf{m}^t), \mathbb{E}[\mathbf{e}^t] \rangle \\ & \quad + \frac{\tau^2 \zeta}{2} \|\nabla L(\mathbf{m}^t)\|_2^2 + \frac{\tau^2 \zeta}{2} \mathbb{E}[\|\mathbf{e}^t\|_2^2] \\ & \quad + \tau^2 \zeta \mathbb{E}[\langle \nabla L(\mathbf{m}^t), \mathbf{e}^t \rangle] \\ & \stackrel{(b)}{=} \frac{-\tau(2-\tau\zeta)}{2} \|\nabla L(\mathbf{m}^t)\|_2^2 + \frac{\tau^2 \zeta}{2} \mathbb{E}[\|\mathbf{e}^t\|_2^2] \\ & \quad + \tau(\tau\zeta - 1) \langle \nabla L(\mathbf{m}^t), \mathbb{E}[\mathbf{e}^t] \rangle \\ & = -\frac{1}{2\zeta} \|\nabla L(\mathbf{m}^t)\|_2^2 + \frac{1}{2\zeta} \mathbb{E}[\|\mathbf{e}^t\|_2^2], \end{aligned} \quad (36)$$

where (a) is from Assumption 2 and (b) is obtained by letting  $\tau = \frac{1}{\zeta}$ . Then, the upper bound of  $\mathbb{E}[\|\mathbf{e}^t\|_2^2]$  is given as follows:

$$\begin{aligned}
& \mathbb{E} \left[ \|\mathbf{e}^t\|_2^2 \right] \\
&= \mathbb{E} \left[ \left\| \frac{1}{|\mathcal{K}|} \sum_{k \in \mathcal{K}} \mathbf{g}_k^t + \frac{1}{|\mathcal{K}|} \mathbf{r}(t) - \nabla L(\mathbf{m}^t) \right\|_2^2 \right] \\
&= \mathbb{E} \left[ \left\| \frac{1}{|\mathcal{K}|} \sum_{k \in \mathcal{K}} \mathbf{g}_k^t - \nabla L(\mathbf{m}^t) \right\|_2^2 \right] + \mathbb{E} \left[ \left\| \frac{1}{|\mathcal{K}|} \mathbf{r}(t) \right\|_2^2 \right] \\
&\quad + \frac{1}{|\mathcal{K}|} \left\langle \frac{1}{|\mathcal{K}|} \sum_{k \in \mathcal{K}} \mathbf{g}_k^t - \nabla L(\mathbf{m}^t), \mathbb{E}[\mathbf{r}(t)] \right\rangle \\
&\stackrel{(a)}{=} \mathbb{E} \left[ \left\| \frac{1}{|\mathcal{K}|} \sum_{k \in \mathcal{K}} \mathbf{g}_k^t - \nabla L(\mathbf{m}^t) \right\|_2^2 \right] + \frac{1}{|\mathcal{K}|^2} \mathbb{E} \left[ \|\mathbf{r}(t)\|_2^2 \right] \\
&= \mathbb{E} \left[ \left\| \frac{1}{|\mathcal{K}|} \sum_{k \in \mathcal{K}} \mathbf{g}_k^t - \nabla L(\mathbf{m}^t) \right\|_2^2 \right] + \frac{d\sigma^2}{|\mathcal{K}|^2 \nu^2} \\
&= \mathbb{E} \left[ \left\| \frac{1}{|\mathcal{K}|} \sum_{k \in \mathcal{K}} \mathbf{g}_k^t - \frac{1}{N} \sum_{k \in \mathcal{K}} \mathbf{g}_k^t - \frac{1}{N} \sum_{k \in \mathcal{N}/\mathcal{K}} \mathbf{g}_k^t \right\|_2^2 \right] + \frac{d\sigma^2}{|\mathcal{K}|^2 \nu^2} \\
&= \mathbb{E} \left[ \left\| \left( \frac{1}{|\mathcal{K}|} - \frac{1}{N} \right) \sum_{k \in \mathcal{K}} \mathbf{g}_k^t - \frac{1}{N} \sum_{k \in \mathcal{N}/\mathcal{K}} \mathbf{g}_k^t \right\|_2^2 \right] + \frac{d\sigma^2}{|\mathcal{K}|^2 \nu^2} \\
&\stackrel{(b)}{\leq} \mathbb{E} \left[ \left( \left( \frac{1}{|\mathcal{K}|} - \frac{1}{N} \right) \sum_{k \in \mathcal{K}} \|\mathbf{g}_k^t\|_2 + \frac{1}{N} \sum_{k \in \mathcal{N}/\mathcal{K}} \|\mathbf{g}_k^t\|_2 \right)^2 \right] \\
&\quad + \frac{d\sigma^2}{|\mathcal{K}|^2 \nu^2} \\
&\stackrel{(c)}{\leq} 4\varpi^2 \left( 1 - \frac{|\mathcal{K}|}{N} \right)^2 + \frac{d\sigma^2}{|\mathcal{K}|^2 \nu^2}, \tag{37}
\end{aligned}$$

where (a) is from the fact that  $\mathbb{E}[\mathbf{r}(t)] = 0$ . Step (b) is achieved by the triangle-inequality and (c) is from Assumption 1. By submitting (37) into (36) and defining  $\eta = 1 - \frac{\varrho}{\zeta}$ , we obtain

$$\begin{aligned}
& \mathbb{E} [L(\mathbf{m}^{t+1}) - L(\mathbf{m}^*)] \\
&\stackrel{(a)}{\leq} \left( 1 - \frac{\varrho}{\zeta} \right) \mathbb{E} [L(\mathbf{m}^t) - L(\mathbf{m}^*)] \\
&\quad + \frac{1}{2\zeta} \left( 4\varpi^2 \left( 1 - \frac{|\mathcal{K}|}{N} \right)^2 + \frac{d\sigma^2}{|\mathcal{K}|^2 \nu^2} \right) \\
&\leq \left( 1 - \frac{\varrho}{\zeta} \right)^t \mathbb{E} [L(\mathbf{m}^0) - L(\mathbf{m}^*)] \\
&\quad + \frac{1}{2\zeta} \left( 4\varpi^2 \left( 1 - \frac{|\mathcal{K}|}{N} \right)^2 + \frac{d\sigma^2}{|\mathcal{K}|^2 \nu^2} \right) \sum_{i=0}^{t-1} \left( 1 - \frac{\varrho}{\zeta} \right)^i \\
&\leq \eta^t \mathbb{E} [L(\mathbf{m}^0) - L(\mathbf{m}^*)] \\
&\quad + \frac{1}{2\zeta} \left( 4\varpi^2 \left( 1 - \frac{|\mathcal{K}|}{N} \right)^2 + \frac{d\sigma^2}{|\mathcal{K}|^2 \nu^2} \right) \frac{1 - \eta^t}{1 - \eta}, \tag{38}
\end{aligned}$$

where (a) is from Assumption 3. Finally, by replacing  $t + 1$  with  $T$ , we complete the proof.

## REFERENCES

- [1] B. McMahan, E. Moore, D. Ramage, S. Hampson, and B. A. y. Arcas, "Communication-efficient learning of deep networks from decentralized data," in *Proc. Int. Conf. Artif. Int. Stat.*, 2017, pp. 1273–1282.
- [2] L. Melis, C. Song, E. De Cristofaro, and V. Shmatikov, "Exploiting unintended feature leakage in collaborative learning," in *Proc. IEEE Symp. Security Privacy*, 2019, pp. 691–706.
- [3] L. Zhu, Z. Liu, and S. Han, "Deep leakage from gradients," in *Proc. Adv. Neural Inf. Process. Syst.*, 2019, pp. 14774–14784.
- [4] P. Kairouz, H. B. McMahan, B. Avent, A. Bellet, M. Bennis, A. N. Bhagoji, K. Bonawitz, Z. Charles, G. Cormode, R. Cummings *et al.*, "Advances and open problems in federated learning," *Found. Trends Mach. Learn.*, vol. 14, no. 1–2, pp. 1–210, 2021.
- [5] K. Yang, T. Jiang, Y. Shi, and Z. Ding, "Federated learning via over-the-air computation," *IEEE Trans. Wireless Commun.*, vol. 19, no. 3, pp. 2022–2035, 2020.
- [6] C. Dwork, A. Roth *et al.*, "The algorithmic foundations of differential privacy," *Found. Trends Theor. Comput. Sci.*, vol. 9, no. 3–4, pp. 211–407, 2014.
- [7] B. Nazer and M. Gastpar, "Computation over multiple-access channels," *IEEE Trans. Inf. Theory*, vol. 53, no. 10, pp. 3498–3516, 2007.
- [8] M. Goldenbaum, H. Boche, and S. Stańczak, "Harnessing interference for analog function computation in wireless sensor networks," *IEEE Trans. Signal Process.*, vol. 61, no. 20, pp. 4893–4906, 2013.
- [9] M. M. Amiri and D. Gündüz, "Machine learning at the wireless edge: Distributed stochastic gradient descent over-the-air," *IEEE Trans. Signal Process.*, vol. 68, pp. 2155–2169, 2020.
- [10] M. Seif, R. Tandon, and M. Li, "Wireless federated learning with local differential privacy," in *Proc. IEEE Int. Symp. Inf. Theory*, 2020, pp. 2604–2609.
- [11] Y. Koda, K. Yamamoto, T. Nishio, and M. Morikura, "Differentially private aircomp federated learning with power adaptation harnessing receiver noise," in *Proc. IEEE Global Communications Conf.*, 2020, pp. 1–6.
- [12] D. Liu and O. Simeone, "Privacy for free: Wireless federated learning via uncoded transmission with adaptive power control," *IEEE J. Sel. Areas Commun.*, vol. 39, no. 1, pp. 170–185, 2020.
- [13] N. Yan, K. Wang, C. Pan, and K. K. Chai, "Private federated learning with misaligned power allocation via over-the-air computation," *IEEE Commun. Lett.*, vol. 26, no. 9, pp. 1994–1998, 2022.
- [14] X. Cao, G. Zhu, J. Xu, Z. Wang, and S. Cui, "Optimized power control design for over-the-air federated edge learning," *IEEE J. Sel. Areas Commun.*, vol. 40, no. 1, pp. 342–358, 2021.
- [15] M. Chen, Z. Yang, W. Saad, C. Yin, H. V. Poor, and S. Cui, "A joint learning and communications framework for federated learning over wireless networks," *IEEE Trans. Wireless Commun.*, vol. 20, no. 1, pp. 269–283, 2020.
- [16] M. P. Friedlander and M. Schmidt, "Hybrid deterministic-stochastic methods for data fitting," *SIAM J. Sci. Comput.*, vol. 34, no. 3, pp. A1380–A1405, 2012.